

Characterization and Modeling of the Al-Oxide/Aqueous Solution Interface

I. Measurement of Electrostatic Potential at the Origin of the Diffuse Layer Using Negative Adsorption of Na^+ Ions

Z. Z. ZHANG,^{*,1} DONALD L. SPARKS,^{*} AND NOEL C. SCRIVNER[†]

^{*} Department of Plant and Soil Sciences, University of Delaware, Newark, Delaware 19717-1303; and [†] Du Pont Engineering, Louviers 1365, Newark, Delaware 19714

Received May 5, 1993; accepted August 10, 1993

A method of measuring electrostatic potential at the origin of the diffuse layer, ψ_d , from co-ion negative adsorption experiments was described and used for an amphoteric Al-oxide. It was found that the magnitude of ψ_d for the Al-oxide decreased with increasing electrolyte concentration. Our data showed that the zeta potential, ζ , differed from ψ_d for the Al-oxide. Therefore, the generally accepted assumption that $\psi_d \approx \zeta$ should be further examined. We modeled our experimental data using the triple layer model. It was shown that both the surface charge density, σ_0 , measured from acid–base titration and ψ_d , determined from co-ion negative adsorption experiments, can be quantitatively described by the triple layer model using a self consistent set of parameters. A major criterion of a desired surface complexation model should be its ability to account for various properties of the interface with a self consistent set of parameters as demonstrated by describing or modeling different experimental data. Hence, further characterization of the physical and chemical nature and properties of the colloidal systems is needed to provide the additional data base for developing, testing, and modifying models. © 1994 Academic Press, Inc.

INTRODUCTION

The electrical properties of the oxide–water interface play an important role in regulating the chemical composition and physical properties of soil–water, sediment–water, and other aquatic systems. For example, specific and nonspecific adsorption of ions, cation and anion exchange, retention and configuration of large organic molecules at the solid–liquid interface, dispersion and flocculation of colloids and thereby, the hydraulic conductivity of soils, and sediments are all affected to some extent by surface charge and potential.

To quantitatively describe chemical reactions occurring in oxides and other amphoteric colloidal surfaces and the

resulting formation of charge and potential, several surface complexation models have been developed in the last two decades. These include: the constant capacitance model (1, 2), the diffuse layer model (3, 4), and the triple layer model (5, 6). The fundamental concepts upon which all surface complexation models are based are essentially the same. These include: (1) surface adsorption takes place at finite and specific coordination sites; (2) surface adsorption reactions can be described by mass action equations; and (3) surface charges and potentials result from and interact with the adsorption reactions. The main differences in these surface complexation models are the manner in which the structure of the interfacial region is described, and the relationships between the charges and potentials at the interfacial regions.

All of the surface complexation models are capable of quantitatively describing both cation and anion adsorption phenomena. Westall and Hohl (7) compared five electrostatic models and found that all models described acid–base titration data for Al_2O_3 and TiO_2 fairly well, with corresponding physical and chemical parameters in the models taking on quite different values for different models. Consequently, Westall and Hohl (7) concluded that these models must be viewed as mathematical descriptions of the data, but they may not necessarily provide an accurate physical description of the interface.

However, an accurate description of the interface is essential to elucidate the mechanisms of surface reactions. In most studies, potentiometric titration methods have been used to determine the surface charge at the oxide–water interface, and the corresponding surface potential can then be calculated according to the model chosen. It is generally accepted that the magnitude of the electrostatic potential at the solid–liquid interface, ψ_0 , is considerably higher than the electrostatic potential at the origin of the diffuse layer, ψ_d . The values of ψ_d for oxides and other colloids were generally

¹ To whom correspondence should be addressed.

inferred from indirect electrophoretic measurements. Lyklema (8) examined the relation between the zeta potential, ζ , and ψ_d estimated from coagulation data on AgI sols and concluded that the two coincide within experimental error. Hunter (9) employed the assumption of $\psi_d \approx \zeta$ in considering the position of the plane of shear. He further suggested that this assumption be adopted for other surfaces, including oxides. However, as Lyklema (8) pointed out, there are practically no systematic studies to compare ψ_d and ζ in the literature to substantiate the reliability of the relation between ψ_d and ζ .

In the present study we will describe a method for determining ψ_d of amphoteric colloids. This method is based on the negative adsorption of co-ions and has been applied to colloids with permanent charge, such as clay minerals (10–12). The main objective of our study was to achieve a better understanding on the nature and properties of the oxide–solution interface and to provide additional sets of experimental data for testing the surface complexation models.

THEORETICAL CONSIDERATIONS

It is well known that amphoteric colloidal particles have net positive charges when $\text{pH} < \text{pH}_{\text{pzc}}$. Therefore, cations such as Na^+ ions should be negatively adsorbed, provided that they are not specifically adsorbed on the surfaces. For planar shaped colloidal particles, the deficit or negative adsorption of Na^+ per unit mass of the colloids, $\Gamma_{\text{Na}}S$, can be found by integrating the difference between C_{Na}^0 , the concentration of Na^+ ions in the external solution, and C_{Na} , the local concentration at any distance, x , from the colloidal surface, over the entire solution volume of the suspension phase, i.e.,

$$\Gamma_{\text{Na}}S = S \int_0^h (C_{\text{Na}}^0 - C_{\text{Na}}) dx, \quad [1]$$

in which S is the specific surface area of the colloidal particles and the upper limit of the integral, and h is the average half distance between the adjacent colloidal particles and is given by V/mS , where V is the volume of the solution in the suspension, and m is the mass of the colloidal particles in the suspension.

The original work of Schofield (13) showed that the negative adsorption of co-ions can be quantitatively described by the diffuse double layer theory. Schofield (13) published an approximation equation for the negative adsorption of co-ions on charged surfaces and demonstrated that his equation can be used to measure S . However, this method of measuring S is based on an additional condition that the surface charge density was sufficiently high such that the concentrations of the co-ions immediately next to the surface approached zero. Van den Hul and Lyklema (14) showed that this condition was equivalent to $\psi_d > 150$ mV. They

also demonstrated that the negative adsorption of co-ions was affected by ψ_d . Although van den Hul and Lyklema (14) provided an equation which related the negative adsorption of co-ions with ψ_d for a 1:2 electrolyte, Chan *et al.* (10) were the first to recognize that the negative adsorption of co-ions can be used to estimate ψ_d and employed this method to determine ψ_d of clay minerals.

In double layer theory it is assumed that the Coulomb attraction and repulsion on the ions in the diffuse layer are counteracted by their thermal motion. The resulting statistical equilibrium is described by the Boltzmann distribution law (15). For Na^+ ions,

$$C_{\text{Na}} = C_{\text{Na}}^0 e^{-e\psi/kT}, \quad [2]$$

in which e is the electronic charge, ψ is the electrostatic potential at distance x from the colloidal surface, k is the Boltzmann constant, and T is the absolute temperature. Substituting Eq. [2] into Eq. [1], one obtains

$$\Gamma_{\text{Na}}S = C_{\text{Na}}^0 S \int_0^h (1 - e^{-e\psi/kT}) dx. \quad [3]$$

In our experiments h was sufficiently large that the double layer was essentially nonoverlapping. Under this condition, the relationship between ψ and x in a 1:1 electrolyte, was given by van Olphen (16) as:

$$e^{-e\psi/kT} = \left(\frac{I - Je^{-\kappa x}}{I + Je^{-\kappa x}} \right)^2, \quad [4]$$

in which $I = e^{e\psi_d/2kT} + 1$, $J = e^{e\psi_d/2kT} - 1$, κ is the Debye–Huckel parameter, given by $\kappa = 3.287 \times 10^7 \sqrt{C^0}$ (cm^{-1}) at 298 K, and C^0 is the equilibrium electrolyte concentration in mol/liter. By substituting Eq. [4] for $e^{-e\psi/kT}$, Eq. [3] can be integrated to yield (17),

$$\Gamma_{\text{Na}}S = \frac{2C_{\text{Na}}^0 S}{\kappa} \left(\frac{2I}{I + Je^{-\kappa h}} - 1 - e^{-e\psi_d/2kT} \right). \quad [5]$$

Since h was large enough such that $\kappa h \gg 1$ and $e^{-\kappa h} \rightarrow 0$, Eq. [5] reduces to the form derived by Chan *et al.* (10), i.e.,

$$\Gamma_{\text{Na}}S = \frac{2C_{\text{Na}}^0 S}{\kappa} (1 - e^{-e\psi_d/2kT}). \quad [6]$$

It is evident from Eq. [6] that the value of ψ_d can be determined from negative adsorption measurements provided S is known. However, it should be noted that the exponent in Eq. [6] differs in sign from that in the equation derived by Chan *et al.* (10). This is because Eq. [6] describes negative adsorption of cations on positively charged colloids, while the equation of Chan *et al.* (10) describes negative adsorption of anions on negatively charged clay surfaces.

MATERIALS AND METHODS

The Al-oxide used in our study was a γ -Al₂O₃ manufactured by the Degussa Corp (Teterboro, NJ), under the name of Aluminum Oxide C. The Al-oxide was suspended in deionized water and the <2 μ m fraction was collected by centrifugation. To remove soluble salts and other impurities, the Al-oxide was dialyzed in deionized water for 7 days, with the deionized water being changed at the beginning and end of each day. Thereafter, the Al-oxide suspension was centrifuged to remove about 50% of the solution. The removed solution was filtered through a minipore filter with a pore size of 0.22 μ m and saved as the reference solution. The remaining Al-oxide was redispersed using a vortex mixer and saved as a suspension. The concentration of the Al-oxide suspension was determined gravimetrically by drying the triplicate samples at 378 K for 24 h. The specific surface area of the Al-oxide was measured by the EGME adsorption method (18).

High-resolution transmission electron microscopy (HRTEM) was employed to examine the shape and morphology of the Al-oxide particles. A dilute suspension sample containing 0.2 mg Al-oxide was dispersed on a holey carbon film supported by a copper mesh grid and air dried at 298 K. The images of the Al-oxide particles were recorded on a Hitachi 9000 NAR transmission electron microscope at 300 kV.

The electrophoretic mobilities of the Al-oxide particles were determined using a ZM 80 Zeta-Meter. The Al-oxide suspension was 0.05% by weight and the background electrolyte (NaCl) ranged from 2.00×10^{-4} to 2.00×10^{-2} M. At least 10 particles were measured and the average electrophoretic mobility was calculated. The ζ potential of the Al-oxide particles was then calculated by using the Smoluchowski equation,

$$\zeta = 4\pi\eta\mu/\epsilon, \quad [7]$$

where μ is the electrophoretic mobility of the particles and η and ϵ are the viscosity and dielectric constant of the liquid, respectively.

To measure the negative adsorption of Na⁺ ions, a set of eight membrane cells similar to those used by Low (19) were constructed out of Plexiglass. A cell consisted of two half cells and each half cell had a central cylindrical slot 1.4 cm deep and 4.0 cm in diameter. One of the half cells was grooved to place an O-ring. The two half cells were held together by four screws with a minipore filter (pore size 0.22 μ m) in between to separate the central cavity into two compartments. Access to the compartments was through holes drilled in the upper edges of the half cells. Two cells were used in a pair, one as a sample cell and the other as a reference. A known amount (by weight) of Al-oxide suspension containing 10 ml of solution (approximately 1 g Al-oxide)

was placed in one compartment of the sample cell and 10 ml of a given NaCl solution was put in the other compartment. The concentrations of NaCl solutions ranged from 4.00×10^{-4} to 4.00×10^{-2} M. In the reference cell, 10 ml of reference solution was placed in one compartment and 10 ml of the same electrolyte solution was put in the other. The cells were covered with parafilms and were shaken on an orbital shaker (Lab-Line Instruments, Inc., Melrose Park, IL) at a speed of 200 RPM for 5 to 7 days until equilibrium was reached. Determinations at each electrolyte concentration were carried out at least in duplicate. The concentrations of Na⁺ ions in the equilibrium solutions in the sample and reference cells were determined using ion chromatography and the negative adsorption of the Na⁺ ions was calculated from the difference between these concentrations.

In our experiments, the values of κ ranged from 5.0×10^5 to 4.7×10^6 cm⁻¹, and $h \approx 7.7 \times 10^{-6}$ cm, with the corresponding κh ranging from 3.8 to 36. Hence, the double layers were essentially nonoverlapping and the boundary conditions used to derive Eq. [4] to [6] were justified. The pH values of the equilibrium solutions were not adjusted. They were within the range of $5.75 < \text{pH} < 6.25$ from the lowest to the highest electrolyte concentrations.

RESULTS AND DISCUSSION

Particle Morphology

The HRTEM images of the Al-oxide particles are shown in Fig. 1. It can be seen clearly that the Al-oxide particles are highly ordered crystalline grains with distinct planar faces. The faceted grains are hexagonal in morphology, with an edge length of approximately 9 nm. The surface areas of these planar faces ranged from 150 to 500 nm². The specific surface area of the Al-oxide, measured by the EGME method, is 130 m²/g.

ζ Potential

The measured values of electrophoretic mobility of the Al-oxide particles at different electrolyte concentrations were converted into ζ potential by using Eq. [7], and the results are presented in Fig. 2. The results showed that the values of ζ potential slightly decreased with increasing electrolyte concentration. However, it is more likely that the decrease in ζ potential is due to the increase in pH associated with increasing electrolyte concentration. It has been reported that ζ potential of montmorillonite is essentially independent of electrolyte concentration (12). The ζ potential of Al-oxide may also behave similarly.

Electrostatic Potential at the Origin of the Diffuse Layer

The measured values of $\Gamma_{\text{Na}}S$ (mmol/g) were divided by C_{Na}^0 (mmol/cm³) and plotted against $2/\kappa$ in Fig. 3. $\Gamma_{\text{Na}}S/C_{\text{Na}}^0$ has the dimension of cm³/g. This term has been

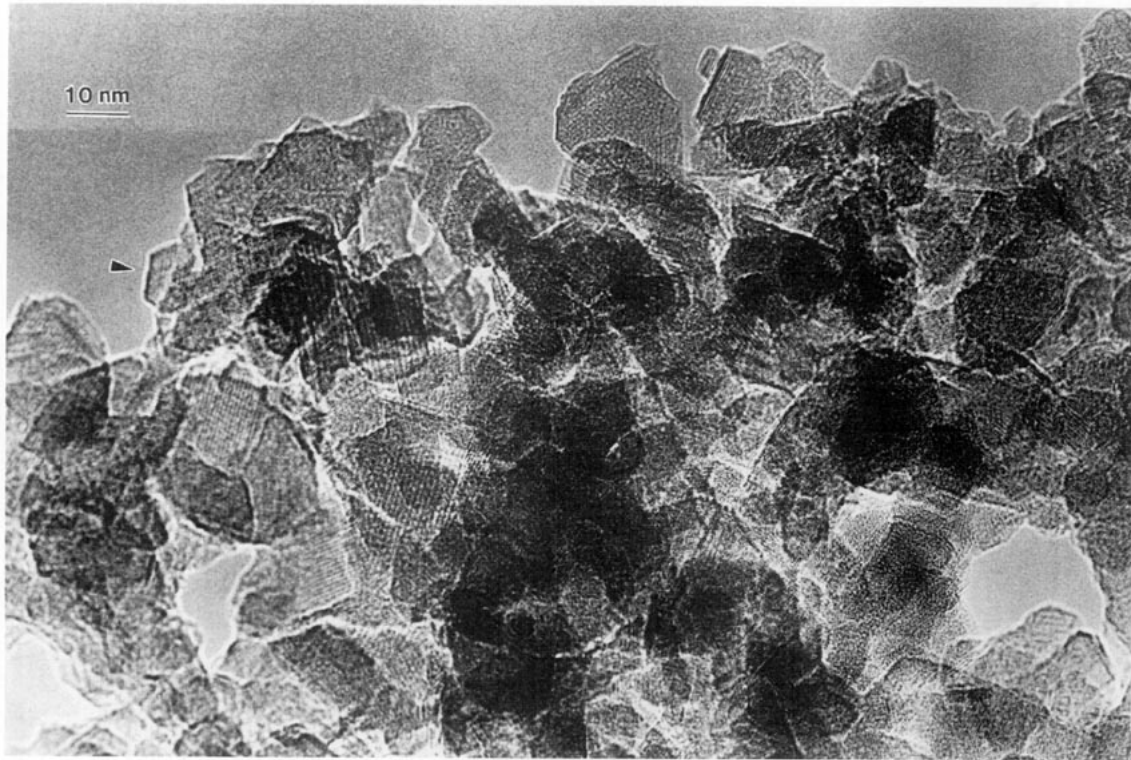


FIG. 1. High-resolution transmission electron microscopy (HRTEM) images of the Al-oxide particles, showing that the particles are highly ordered crystalline grains with distinct planar faces. The faceted grains are hexagonal in morphology, with an edge length of approximately 9 nm (see the arrow).

referred as the exclusion volume in the literature (10–13). Physically, the exclusion volume is the equivalent volume per unit mass of colloidal particles, from which the co-ions are completely excluded. In other words, the exclusion volume is the difference between the volume of the solution and the volume the co-ions would occupy if they were uniformly distributed at a constant concentration of the external solution (11). According to Eq. [6], a linear relationship would result if ψ_d is independent of electrolyte concentration.

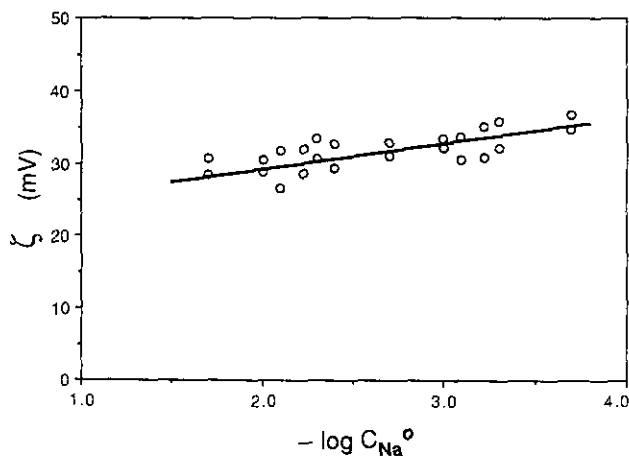


FIG. 2. Values of ζ potential of Al-oxide at different NaCl concentrations.

Our data clearly showed that the relationship is curvilinear, hence ψ_d of an amphoteric colloid is affected by the electrolyte concentration. We solved Eq. [6] for each of the individual negative adsorption datum to determine the values of ψ_d for the Al-oxide. The results are presented in Fig. 4. The values of ψ_d are scattered, since $\Gamma_{Na}S$ is related to the exponential of ψ_d . A small variation in the experimental values of $\Gamma_{Na}S$

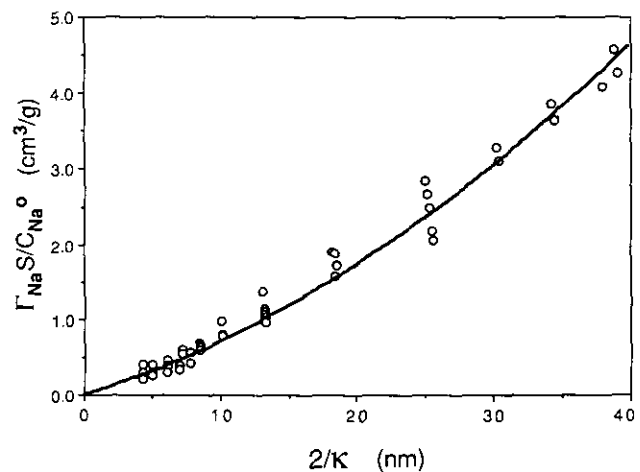


FIG. 3. Measured negative adsorption of Na^+ ions (expressed as exclusion volume) as a function of $2/\kappa$.

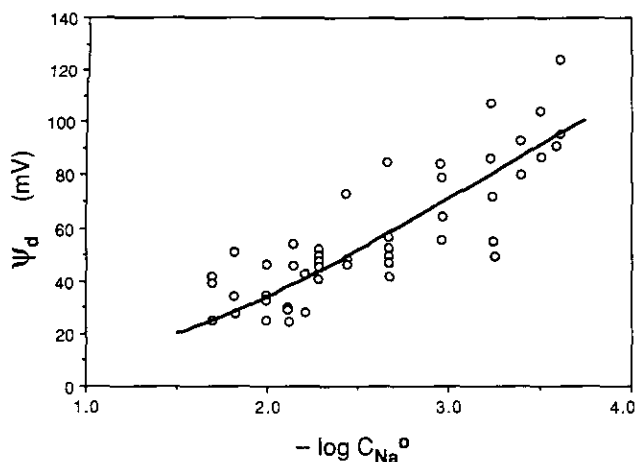


FIG. 4. Values of ψ_d for Al-oxide from Na^+ negative adsorption measurements at different NaCl concentrations. The solid line represents the triple layer modeling of ψ_d as related to equilibrium electrolyte concentration.

would result in a large change in the calculated values of ψ_d . Unfortunately, this is an intrinsic disadvantage of the method. The data show that ψ_d decreased with increasing electrolyte concentration. This decrease in ψ_d is likely due to an increase in adsorption of counterions at the interface. In contrast to amphoteric Al-oxide, the values of ψ_d for illite and montmorillonite depended on the nature of the adsorbed cations but were independent of the electrolyte concentration (10–12). In addition, the data in Figs. 2 and 4 showed that the ζ potential differed from ψ_d . This result is contrary to the findings of Lyklema on AgI (8) and Miller and Low (12), who found that for montmorillonite the ζ potential and ψ_d coincided with each other within experimental error.

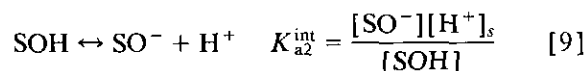
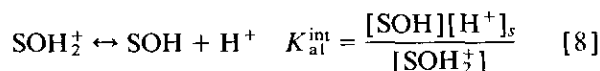
It is well known that the acid-base equilibrium of amphoteric colloidal surfaces is affected by the background electrolyte. This is because increases in the concentration of background electrolyte cause additional binding of counterions to the surface charge sites and this in turn is accompanied by adsorption or desorption of protons, depending on whether the pH is below or above the ZPC (5, 6). In addition, studies of electrophoretic potential and colloid stability have suggested that the magnitude of the diffuse layer charge rarely exceeds 20% of that of the surface charge (5, 20, 21). Therefore, to maintain electroneutrality, there must be a region where the counterions accumulate to neutralize the remaining charge.

In view of the above experimental evidence, both the diffuse layer model and the constant capacitance model do not give a complete description of the solid-liquid interface, since the former model assumes that the total charge is neutralized by the diffuse charge, while the latter assumes the absence of a diffuse layer. The triple layer model, however, gives a much better description of the interface. It allows for the existence of both a diffuse layer and a compact layer in which counter ions accumulate. Physically, the triple layer model

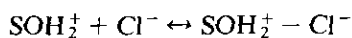
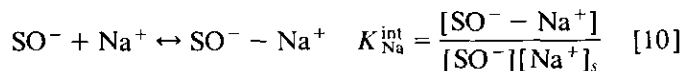
consists of two constant capacitance layers and a diffuse layer (6). We wanted to determine if this model could be used to describe our data of ψ_d .

Model Formulations

The model formulations presented here followed that of Davis *et al.* (6). The amphoteric ionization reactions on the surfaces of Al-oxide can be described by



where K_{a1}^{int} and K_{a2}^{int} can be considered as the first and second acidity constants of the surfaces, and the subscript s denotes concentration on the surfaces. Since these constants are formulated using the surface concentration of protons, they are referred to as intrinsic constants. To account for the adsorption of the counterions, Yates *et al.* (5) proposed the formation of “ion pairs” at charged surface sites,

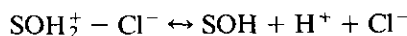


$$K_{\text{Cl}}^{\text{int}} = \frac{[\text{SOH}_2^+ - \text{Cl}^-]}{[\text{SOH}_2^+][\text{Cl}^-]_s} \quad [11]$$

Davis *et al.* (6) showed that for the purpose of computation the above ion pair formation reactions may be written as complex ionization reactions,



$$K_{\text{Na}}^{\text{int}} = \frac{[\text{SO}^- - \text{Na}^+][\text{H}^+]_s}{[\text{SOH}][\text{Na}^+]_s} \quad [12]$$



$$K_{\text{Cl}}^{\text{int}} = \frac{[\text{SOH}][\text{H}^+]_s[\text{Cl}^-]_s}{[\text{SOH}_2^+ - \text{Cl}^-]} \quad [13]$$

The charge density at the solid-solution interface, σ_0 , and the charge density in the β layer (where counterions are adsorbed), σ_β , are given by

$$\sigma_0 = B([\text{SOH}_2^+] + [\text{SOH}_2^+ - \text{Cl}^-] - [\text{SO}^-] - [\text{SO}^- - \text{Na}^+]) \quad [14]$$

$$\sigma_\beta = B([\text{SO}^- - \text{Na}^+] - [\text{SOH}_2^+ - \text{Cl}^-]) \quad [15]$$

where B is a constant that converts surface charge from mol/liter to Coulomb/m², and $B = F/C_s S$, in which F is the Faraday constant and C_s is the Al-oxide concentration in the suspension. The charge density at the origin of the diffuse layer, σ_d , is given by the electroneutrality relationship:

$$\sigma_0 + \sigma_\beta + \sigma_d = 0. \quad [16]$$

The number of surface sites per unit surface area, N_s , can be written as,

$$N_s = \frac{N}{C_s S} ([\text{SOH}] + [\text{SOH}_2^+] + [\text{SOH}_2^+ - \text{Cl}^-] + [\text{SO}^-] + [\text{SO}^- + \text{Na}^+]), \quad [17]$$

where N is Avogadro's number.

The charge-potential relationships are as follows:

$$\sigma_0 = C_1(\psi_0 - \psi_\beta) \quad [18]$$

$$\sigma_d = -C_2(\psi_\beta - \psi_d) \quad [19]$$

$$\sigma_d = -0.1174\sqrt{C^0}\sinh(e\psi_d/2kT), \quad [20]$$

where C_1 and C_2 are the inner and outer layer capacitances, respectively.

Determination of the model parameters

The surface acidity and surface complex constants were determined using the double extrapolation method introduced by James *et al.* (22) and the titration data of Schulthess and Sparks (23). The resulting values are: $\text{p}K_{\text{a1}}^{\text{int}} = 5.6$, $\text{p}K_{\text{a2}}^{\text{int}} = 11.6$, $\text{p}K_{\text{Na}}^{\text{int}} = 10.2$, and $\text{p}K_{\text{Cl}}^{\text{int}} = 7.1$. Similar data were reported by Huang (24) and James and Parks (25).

The values of N_s for oxides range from 2 to 20 sites/nm² (25). Pieper and de Vooy (26) reported a C_2 value of 0.2 F/m² ($F = C/\text{volt}$) from direct measurements on the AgI electrolyte interface. In our modeling, we have used a value of 6 sites/nm². The outer layer capacitance, C_2 , was assumed to be 0.2 F/m². The inner layer capacitance, C_1 , was treated as an adjustable parameter. Based on a consideration of the dielectric constant in the interfacial region and the closest approach of a hydrated monovalent ion to the surface, Hayes *et al.* (27) concluded that C_1 should be within the range of 0.1 to 2.0 F/m².

Modeling Results

Borkovec and Westall (28) have formulated a solution of the surface excesses of ions in the diffuse layer using matrix equations. The matrix notation is also employed in several computer algorithms such as MINEQL, MICROQL, and MINTEQ. The main benefits of the matrix equations are the generality of the notation and the computational advan-

tage associated with it. For our purpose of model testing, we decided to express the model in terms of explicit symbolic equations. We incorporated the triple layer model into the TK Solver Program (Universal Technical Systems, Inc., Rockford, IL). This program is a high-level computer program for solving sets of algebraic equations and for tabulating and plotting the results (29). In the TK Solver environment, equations are viewed as relationships or rules, not as assignment statements. The TK Program has both a direct solver, which solves the sets of equations using a consecutive substitution procedure, and an iterative solver, which employs a modified Newton-Raphson method. When using the iterative solver, the user needs to assign a guess status to one or more variables and to provide reasonable initial guesses for these variables.

We set up the triple layer model as a set of 11 equations with 11 unknowns, namely, $[\text{SOH}]$, $[\text{SOH}_2^+]$, $[\text{SOH}_2^+ - \text{Cl}^-]$, $[\text{SO}^-]$, $[\text{SO}^- + \text{Na}^+]$, σ_0 , σ_β , σ_d , ψ_0 , ψ_β , and ψ_d . The known variables or parameters are pH, C^0 , $K_{\text{a1}}^{\text{int}}$, $K_{\text{a2}}^{\text{int}}$, $K_{\text{Na}}^{\text{int}}$, $K_{\text{Cl}}^{\text{int}}$, C_1 , C_2 , and N_s . The rule sheet for the triple layer model is shown in Table 1. The electrostatic potential ψ is expressed as the dimensionless "reduced potential," y , defined as $y = e\psi/kT$. The constant 38.914 in the potential-charge relationship equations is a conversion factor between the reduced potential and the volt. The pH was in the range of $5.75 < \text{pH} < 6.25$ for the lowest to the highest electrolyte

TABLE 1
The Rule Sheet of TK Solver Model Oxide.tk

$\text{SOH}_2 = \text{SOH} \cdot \text{H} \cdot \exp(-y_0)/K_1$	Mass action eq. for SOH_2
$\text{SO} = \text{SOH} \cdot \exp(y_0) \cdot K_2/\text{H}$	Mass action eq. for SO
$\text{SONa} = \text{SOH} \cdot \text{Na} \cdot \exp(y_0 - y_\beta) \cdot K_{\text{Na}}^{\text{int}}/\text{H}$	Mass action eq. for SONa
$\text{SOH}_2\text{Cl} = \text{SOH} \cdot \text{H} \cdot \text{Cl} \cdot \exp(y_\beta - y_0)/K_{\text{Cl}}^{\text{int}}$	Mass action eq. for SOH_2Cl
$N_s = B \cdot (\text{SOH}_2 + \text{SOH} + \text{SO} + \text{SOH}_2\text{Cl} + \text{SONa})$	Mass balance eq.
$\sigma_0 = B \cdot (\text{SOH}_2 + \text{SOH}_2\text{Cl} - \text{SO} - \text{SONa})$	Charge at surface
$\sigma_\beta = B \cdot (\text{SONa} - \text{SOH}_2\text{Cl})$	Charge in compact layer
$\sigma_0 + \sigma_\beta + \sigma_d = 0$	Charge balance eq.
$y_0 = y_\beta + \sigma_0 \cdot 38.914/C_1$	Potential at surface
$y_\beta = y_d - \sigma_d \cdot 38.914/C_2$	Potential at compact layer
$\sigma_d = -11.74 \cdot \sqrt{C^0} \cdot \sinh(y_d/2)$	Potential at diffuse layer
$\text{pH} = -\log(\text{H})$	Definition of pH
$\text{p}C^0 = -\log(C^0)$	Definition of $\text{p}C^0$
$\text{p}K_1 = -\log(K_1)$	Definition of $\text{p}K_1$
$\text{p}K_2 = -\log(K_2)$	Definition of $\text{p}K_2$
$\text{p}K_{\text{Na}}^{\text{int}} = -\log(K_{\text{Na}}^{\text{int}})$	Definition of $\text{p}K_{\text{Na}}^{\text{int}}$
$\text{p}K_{\text{Cl}}^{\text{int}} = -\log(K_{\text{Cl}}^{\text{int}})$	Definition of $\text{p}K_{\text{Cl}}^{\text{int}}$
$C_s = M/V$	Conc. of Al-oxide, g/ml
$A1 = 1000 \cdot C_s \cdot A$	Surface area, m ² /liter
$B = 1E6 \cdot F/A1$	Conversion factor mol/liter to F/m ²
$\text{Na} = C^0$	Equilibrium conc. of Na
$\text{Cl} = C^0$	Equilibrium conc. of Cl
$\text{pH} = 6.5 - 0.2 \cdot \text{p}C^0$	Conc. and pH relationship

concentrations. We found that the relationship between pH and electrolyte concentration can be approximated by $\text{pH} \approx 6.5 - 0.2\text{p}C_{\text{eq}}$.

To run the iterative solver, it was necessary to assign a guess status to at least three variables. We selected to provide initial guesses for $[\text{SOH}]$, $[\text{SOH}_2^+]$, and ψ_d . It is conceivable that the majority of the sites should be in the neutral form, hence $[\text{SOH}]$ was given an initial value of 0.15 M , which is equivalent to approximately 6 sites/nm^2 , $[\text{SOH}_2^+]$ was given an initial value of 0.0001 M , and ψ_d was guessed to be 10 mV . The TK Solver program allows us to model all of the unknowns listed above. In addition, sensitivity analyses with respect to any known variables or parameters can be easily performed.

We have modeled the values of both σ_0 and ψ_d for $C_1 = 1.2, 1.4, \text{ and } 1.6 \text{ F/m}^2$. Since the values of σ_0 were very sensitive to changes in C_1 , while the values of ψ_d were insensitive, the value of C_1 was adjusted based on the σ_0 data. It was found that the best fit for the acid-base titration data of Schulthess and Sparks (23) was obtained when $C_1 = 1.4 \text{ F/m}^2$ (Fig. 5). The modeling results for ψ_d are presented in Fig. 4 in comparison to the experimental data. It is clear that the triple layer model quantitatively described the experimental data for σ_0 versus pH and ψ_d as related to electrolyte concentration. Earlier investigators have shown that the triple layer model successfully modeled adsorption data for alkali and alkaline earth metal cations (25, 30), trace metal cations (31–33), and anion ligands (34–36). Therefore, the general validity of the triple layer model has been well established.

It is well recognized that the fit of a model with a particular property or a given set of experimental data of the interface does not necessarily prove that the model is correct physically. This may simply be due to the fact that the particular property of the interface is not sensitive to the deficiency of the model. For example, the specific adsorption of ions on

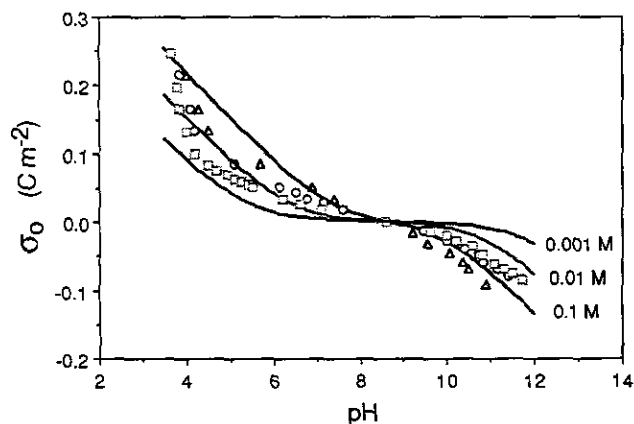


FIG. 5. Triple layer modeling of σ_0 for Al-oxide measured from acid-base titration as a function of pH and electrolyte concentration (Data from Ref. (23)).

surfaces is not very sensitive to the existence of the diffuse layer, so that the constant capacitance model has been successfully used to describe such experimental data (37–39). However, if a model can successfully describe several properties of the interface, it is likely that the deficiencies of the model are diminished. Therefore, further characterization of the nature and properties of the interfaces is essential if one wishes to obtain physically reliable models.

SUMMARY

In summary, we have measured ψ_d for an Al-oxide as affected by the equilibrium electrolyte concentration using negative adsorption of Na^+ ions. It was found that the magnitude of ψ_d for the amphoteric Al-oxide decreased with increasing electrolyte concentration. Our data showed that the ζ potential differed from ψ_d for the Al-oxide, therefore, the generally accepted assumption that $\psi_d \approx \zeta$ should be further examined. It was shown that both σ_0 , measured from acid-base titration, and ψ_d , determined from negative adsorption experiments, can be quantitatively described by the triple layer model using a self-consistent set of parameters. A major criterion of a desired surface complexation model should be its ability to account for different properties of the interface with a self-consistent set of parameters. Hence, further characterization of the physical and chemical nature and properties of the colloidal systems is needed to provide the additional data base for developing, testing, and verifying models.

ACKNOWLEDGMENTS

The authors thank the Du Pont Company for financial support of this research. The authors also are grateful to Dr. Scott Fendorf for conducting the HRTEM image analysis of the Al-oxide, Ms. Caroline Golt for the ion chromatography analysis, Dr. Paul Grossl for determining the surface area of the Al-oxide, and Mr. Gerald Hendricks for his laboratory assistance.

REFERENCES

1. Schindler, P. W., in "Adsorption of Inorganics at Solid-Liquid Interfaces" (M. A. Anderson and A. J. Rubin, Eds.), Ann Arbor Science, Ann Arbor, MI, 1981.
2. Schindler, P. W., and Gamsjager, H., *Kolloid Z. Z. Polym.* **250**, 759 (1972).
3. Stumm, W., Huang, C. P., and Jenkins, S. R., *Croat. Chem. Acta* **42**, 223 (1970).
4. Huang, C. P., and Stumm, W., *J. Colloid Interface Sci.* **43**, 409 (1973).
5. Yates, D. E., Levine, S., and Healy, T. W., *J. Chem. Soc. Faraday Trans. 1.* **70**, 1807 (1974).
6. Davis, J. A., James, R. O., and Leckie, J. O., *J. Colloid Interface Sci.* **63**, 480 (1978).
7. Westall, J., and Hohl, H., *Adv. Colloid Interface Sci.* **12**, 265 (1980).
8. Lyklema, J., *J. Colloid Interface Sci.* **58**, 242 (1977).
9. Hunter, R. J., "Zeta Potential in Colloid Science: Principles and Applications." Academic Press, New York, 1981.
10. Chan, D. Y. C., Pashley, R. M., and Quirk, J. P., *Clays Clay Miner.* **32**, 131 (1984).

11. Zhang, Z. Z., "Interaction of water and organic compounds with clay as determined from heat of immersion and heat of adsorption." Ph.D. thesis, Purdue University, 1988.
12. Miller, S. E., and Low, P. F., *Langmuir* **6**, 572 (1990).
13. Schofield, R. K., *Nature* **160**, 408 (1947).
14. Van den Hul, H. J., and Lyklema, J., *J. Colloid Interface Sci.* **23**, 500 (1967).
15. Verway, E. J. W., and Overbeek, J. Th. G., "Theory of the Stability of Lyophobic Colloids." Elsevier, New York 1948.
16. Van Olphen, H., "An Introduction to Clay Colloid Chemistry", Wiley-Interscience, New York, 1974.
17. Stone, A. T., *J. Colloid Interface Sci.* **127**, 429 (1989).
18. Carter, D. L., Heilman, M. D., and Gonzalez, C. L., *Soil Sci.* **100**, 356 (1965).
19. Low, P. F., *Soil Sci.* **77**, 29 (1954).
20. Breeuwsma, A., and Lyklema, J. J., *Discuss. Faraday Soc.* **52**, 324 (1971).
21. Breeuwsma, A., and Lyklema, J., *J. Colloid Interface Sci.* **43**, 437 (1973).
22. James, R. O., Davis, J. A., and Leckie, J. O., *J. Colloid Interface Sci.* **65**, 331 (1978).
23. Schulthess, C. P., and Sparks, D. L., *Soil Sci. Soc. Am. J.* **50**, 1406 (1986).
24. Huang, C. P., in "Adsorption of Inorganics at Solid-Liquid Interfaces" (M. A. Anderson and A. J. Rubin, Eds.), Ann Arbor Science, Ann Arbor, 1981.
25. James, R. O., and Parks, G. A., *Surf. Colloid Sci.* **12**, 119 (1982).
26. Pieper, J. H. A., and de Vooy, D. A., *J. Electroanal. Chem.* **53**, 243 (1974).
27. Hayes, K. F., Ela, G. W., and Leckie, J. O., *J. Colloid Interface Sci.* **142**, 448 (1991).
28. Borkovec, M., and Westall, J., *J. Electroanal. Chem.* **150**, 325 (1983).
29. Smith, A. L., in "Artificial Intelligence Applications in Chemistry" (T. H. Pierce and B. A. Hohne, Eds.), ACS Symposium Series, No. 306, Amer. Chem. Soc., Washington, DC, 1986.
30. Wiese, G. R., "Cation Adsorption and Heterocoagulation in Oxide/Water Systems", Ph.D. thesis, University of Melbourne, 1976.
31. Davis, J. A., and Leckie, J. O., *J. Colloid Interface Sci.* **74**, 32 (1980).
32. Fu, G., Allen, H. E., and Cowan, C. E., *Soil Sci.* **152**, 72 (1991).
33. Hayes, K. F., and Leckie, J. O., *J. Colloid Interface Sci.* **115**, 546 (1987).
34. Zhang, P. C., and Sparks, D. L., *Soil Sci. Soc. Am. J.* **53**, 1028 (1989).
35. Zhang, P. C., and Sparks, D. L., *Soil Sci. Soc. Am. J.* **54**, 1266 (1990).
36. Zhang, P. C., and Sparks, D. L., *Environ. Sci. Technol.* **24**, 1848 (1990).
37. Goldberg, S., and Sposito, G., *Soil Sci. Soc. Am. J.* **48**, 772 (1984).
38. Goldberg, S., and Sposito, G., *Soil Sci. Soc. Am. J.* **48**, 779 (1984).
39. Goldberg, S., *Soil Sci. Soc. Am. J.* **496**, 851 (1985).